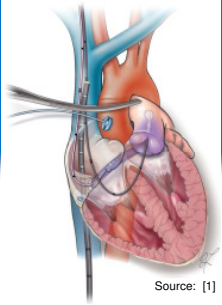


Impact of the thickness of the aortic wall during cross-clamping

STUDENT PROJECT
Computational Bioengineering
Praktikum SS2012

Christoph Hannich¹, Claudia Wittkowske¹

¹ Institute for Computational Mechanics, Technische Universität München, Germany



Source: [1]

Introduction

Cross-clamping of the aorta is routinely performed during cardiac surgery. Alone in the U.S. this procedure is performed in about half million patients per year [2]. For instance, during cardiopulmonary bypass surgery, the aorta needs to be closed off by cross-clamping to keep the heart bloodless [3]. Clamping can cause various degrees of damage to the artery from endothelium delamination to severe intima injury [4]. The stresses and strains of the aortic wall can be indicators for the damage induced to the artery during this procedure. In current simulations a constant wall thickness is assumed. However, the thickness of the aorta varies from patient to patient. The objective of this study was to simulate cross-clamping of the aorta with different wall thickness. It aims to clarify the influence of the thickness of the aortic wall on stresses and strains. These results can provide valuable information about the potential degree of damage to the aorta during cross-clamping depending on the patient-specific wall thickness and can also lead to improvements of the design of aortic clamps.

Methods



Figure 1. CT scan with the segmented aorta (shown in red).

Segmentation

The lumen of the ascending aorta of a patient (male, 70 years) was segmented and reasonably smoothed using Mimics (Materialise). Different methods commonly applied in image segmentation including

- Thresholding
- Cropping
- Region Growing
- Editing Masks and
- Morphology Operations (Erode, Dilate, Open, Close)

were utilized for the segmentation (Figure 1).

Meshing

A tetragonal mesh was created using Cubit (Sandia Corporation). Based on this mesh, aortic walls were extruded with different thickness (1.8 mm, 2.3 mm and 2.8 mm) utilizing a wall-extrude algorithm which enhanced the outer lumen. The created hexagonal finite element mesh consisted of three layers. DeBaKey clamps which are typically used for cross-clamping were simulated by rectangular bars (4x2x60 mm) in Cubit. The clamps were placed 24mm away from the centreline of the artery and facing each other. Clamping occurred perpendicular to the centreline of the aorta. An extruded aorta mesh with open cross-clamps is depicted in Figure 2. Node sets were defined in ICFM CFD (Ansys).

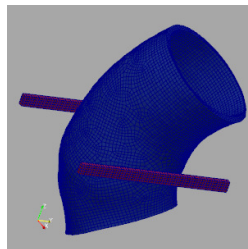


Figure 2. Extruded and meshed aorta segment (blue) with clamps (red). The aortic wall had a thickness of 1.8mm and consists of three layers

Boundary Conditions (BC)

Contact conditions were assigned between the outer surface of the ascending aorta wall and the inner surfaces of the clamps. The boundary of the wall was fixed with Dirichlet BC. The clamp movement was described as a linear movement of 16 mm per second. During the clamp movement the aorta was under the constant blood pressure of 60 mmHg.

Finite Element Solver and Post Processing

An input file containing the mesh information, boundary conditions and solver settings was created to use with the in-house finite element solver 'baci'. The neo-Hookean model by Raghavan and Vorp [5] was applied for the simulation of the aortic wall material. Clamps were modelled with an isotropic material model (Young's modulus 210 GPa).

The segmented geometry was reconstructed from in vivo CT scans and therefore represented a deformed configuration stressed by typical in vivo conditions [6]. Taking this into account the aortic wall was pre-stressed for the first 0.3 seconds with orthogonal diastolic blood pressure of 60mmHg (Figure 3). During the rest of the simulation the pressure was kept constant. Results were post-processed using Paraview.

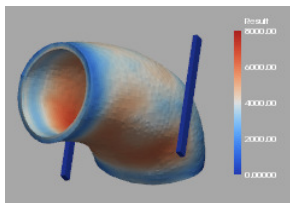


Figure 3. Aorta Segment after pre-stressing with von Mises stress distribution.

Results

All models did not reach complete occlusion and difficulties in achieving convergence appeared when the vessels were highly deformed. The times when the simulations aborted are shown in Table 1.

Wall Thickness [mm]	1.8	2.3	2.8
Time [s]	1.75	1.67	1.57

Table 1: Time length of simulation until abortion because of lacking convergence. The simulation with the thickest aorta wall aborted first after 1.57 sec.

The von Mises stress distribution is similar in all the three models. The highest stress appeared on the inside of the wall in the inner bend. Another increase of the stress level could be seen where the wall folds because of the clamping. On the outer bend no high stress levels were induced. The boundary conditions, in particular the fixation of the wall, also influenced the von Mises stress distribution as depicted in Figure 4.

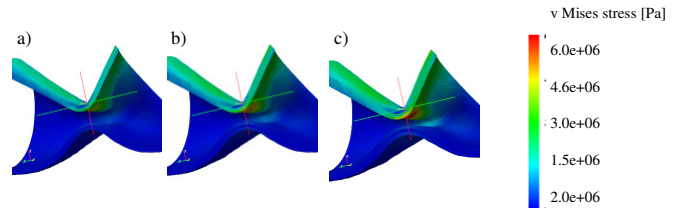


Figure 4. Distribution of von Mises stress on the aortic vessel after 1.57sec of cross-clamping. The highest stress was induced on the inner bend on the inside of the wall. Clamps are not shown. The thickness of the aortic wall varied (a) 1.8mm, b) 2.3mm, c) 2.8mm).

To observe the stress development over time in the three different aorta models, the cell with the highest induced von Mises stress was selected and the development of the von Mises stress was plotted (Figure 5). The maximum stress ($\sigma_{max}=6.27e+07$ Pa) did not depend on the thickness of the wall. However, the increase in stress and the maximum stress level could be observed earlier in a thicker aorta wall. This means that at specific points in time thicker aortic walls were always under higher pressure compared to thinner aortic walls.

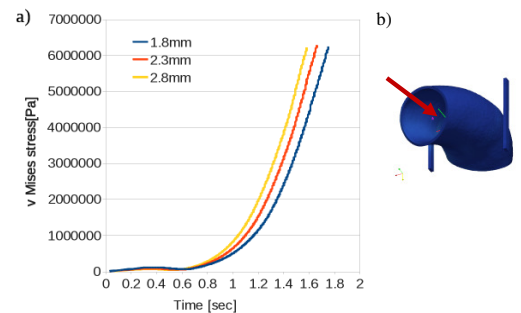


Figure 5. Development of von Mises stress over time when observing the cell under maximum stress. a) Plot of the von Mises stress in a selected cell over time. The influence of the thickness of the aortic vessel on the shape of the curves was very limited. The maximum stress level was reached earlier in a thicker vessel. b) The red arrow points to the location of the cell with the maximum von Mises stresses after 1.57sec of cross-clamping.

The third principal strains were the largest principal strains in this simulation which are shown in Figure 6. The strain distribution was very similar in all aortic walls. The biggest third principal strain after 1.57 sec of cross-clamping was 0.28 and appeared in the aortic wall with a thickness of 2.8mm.

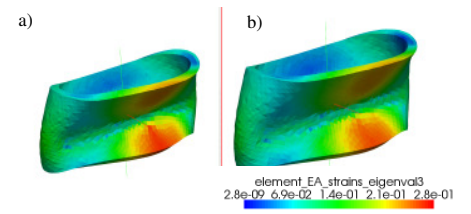


Figure 6. Third principal strains in aortic wall after 1.57 sec of cross-clamping. The thickness of the vessels varied a) 2.3mm and b) 2.8mm.

Conclusion

The influence of the thickness of aortic walls on stresses and strains was very small. The thickness appeared to have no influence on the maximum stress level.

The earlier rise in the stress level of the thicker aortic wall could also have been influenced by the fact that the thicker walls were earlier in contact with the clamps than the thinner walls. Therefore, it would be interesting to observe the behaviour when the clamps are placed at the same distance from the vessel wall. In addition, the boundary conditions had a strong influence on the stress distribution. In future projects the segmented part of the aorta should be longer to decrease the impact of these boundary conditions.

Strains bigger than 0.3 can lead to damages in the aortic vessels. Since the maximum strains in all aortic vessels appeared to be smaller than 0.3, it can be concluded that cross-clamping to this point will not cause any damage to the vessel. However, all vessels were not completely occluded at that point.

In the future, the boundary conditions and potentially the size of the elements have to be improved in order to reach complete occlusion.

This model proved to be very useful in predicting stresses and strains for cross-clamping of aortic vessels. Future research needs to aim at developing a reliable damage criterion.

REFERENCES:

- [1] T. Mihaljevic, A. Gillinov, C. Jarrett, L. Seto, R. Savage, P. DeVilliers (2009), Endoscopic robotically-assisted mitral valve repair, Multimedia Manual of Cardio-Thoracic Surgery, 0914
- [2] H. Chen, J. Navia, G. Kassab (2009), A Simulation of Vessel-Clamp Interaction: Transient Closure Dynamics, Annals of Biomedical Engineering, 37:1772-1780
- [3] S. Gelman (1995), The Pathophysiology of Aortic Cross-clamping and Unclamping, Anesthesiology, 82:1026-1057
- [4] U. von Oppel, T. Dunne, M. De Groot, P. Zilla (1994), Traumatic aortic rupture: Twenty-year metaanalysis of mortality and risk of paraplegia, The Annals of Thoracic Surgery, 58: 585-593.
- [5] M. Raghavan, D. Vorp, (2000), Toward a biomechanical tool to evaluate rupture potential of abdominal aortic aneurysm: identification of a finite strain constitutive model and evaluation of its applicability, J. Biom., 33: 475-482.
- [6] M. W. Gee, Ch. Förster, W. A. Wall (2009), A computational strategy for prestressing patient specific biomechanical problems under finite deformation, Comm. Numerical Methods in Engineering, DOI: 10.1002/cnm.1236